Int. J. Solids Structures Vol. 29, No. 6, pp. 669–688, 1992
Printed in Great Britain.
0020-7683/92 $5.00 + .00

MECHANICS OF SUBINTERFACE CRACKS IN LAYERED MATERIAL

H. LU and T. J. LARDNER
Department of Civil Engineering, University of Massachusetts, Amherst, U.S.A.

(*Received* 13 *March* 1991 ; *in revised form* 10 *June* 1991)

Abstract—Two-dimensional finite cracks near a bi-material interface are investigated. A crack under uniform pressure or a pair of concentrated loads on its faces is modeled by a dislocation density along the crack length leading to singular integral equations from which the stress intensity factors are obtained. We investigated the case when the crack is near the interface of two half-planes or near a finite coating. In both cases, the singular integral equations were solved numerically by expanding the unknown dislocation density in terms of Chebyshev polynomials.

When the crack is near the interface of two half-planes, the stress intensity factors and the energy release rate were obtained as a function of the crack-to-interface distance, and we show that they approach previously derived asymptotic solutions.

When the crack is near the interface of a coated substrate we find in the case of soft coating, for all values of the thickness of the coating and the crack-to-interface distance that the normalized Mode I stress intensity factor and the normalized energy release rate are greater than one, and the normalized stress intensity factor for Mode II is negative. As a result, a soft coating does not prevent a crack propagating toward the interface. On the other hand, for a stiff coating, whether the normalized Mode I stress intensity factor and the normalized energy release rate are greater or less than one, and whether the normalized Mode II stress intensity is positive or negative depends on the relative values of the material stiffness, the crack-to-interface distance, and the thickness of the coating. For this case the critical thickness of the coating for the crack to propagate parallel to the interface was obtained. We also investigated the effect of the value of the material mismatch parameters on the stress intensity factors and the energy release rate.

1. INTRODUCTION

The bonding of different materials is widely used in industry for adhesive joints, fiber-reinforced materials, coating/substrate systems, ceramic/metal systems and the like, and manufacturing imperfections in bonding usually appear as inclusions, flaws or cracks near or on the bonded interfaces. These imperfections create stress concentrations and may lead to delamination of a coating from a substrate, pull out of fibers in a fiber-reinforced matrix, failure of an adhesive joint, etc. In view of its importance in the behavior of a bonded structural component, the problem of an interface crack has given rise to a large number of studies in order to understand the failure process of the interface.

Williams (1959), Malyshev and Salganik (1965), England (1965), Rice and Sih (1965), Cherepanov (1979) and Erdogan (1963, 1965) were among the original investigators of interface crack problems; a recent overview of the analysis of interface cracks can be found in Rice (1988), Comninou (1990) and Lu and Lardner (1991). In addition to cracks along an interface, cracks approaching, parallel to, or terminating at an interface have also been considered by several investigators [see e.g. Bogy (1971), Erdogan and Arin (1975), Ashbaugh (1975), Fenner (1976), Comninou (1979), Lu and Erdogan (1983a, b), He and Hutchinson (1989) and Chen (1991)].

The application of dislocation singularities to crack problems has provided simplifications in the formulation and solution of many crack problems (Rice, 1968; Bilby and Eshelby, 1968). The approach is to model a crack by continuously distributed dislocations described by a density function (Thouless *et al.*, 1987; Hutchinson *et al.*, 1987; He and Hutchinson, 1988, 1989; Suo and Hutchinson, 1989a, b, 1990; Hutchinson and Suo, 1991) and to solve the resulting singular integral equation numerically.

The objective of this paper is to investigate cracks near and parallel to an interface under uniform pressure or a pair of concentrated loads. The interest in cracks under a pair of concentrated loads is motivated by the use of indentation fracture mechanics to investigate the fracture toughness of interfaces (Ostojic and McPherson, 1987; Cook and Pharr, 1990; Evans *et al.*, 1986; Lardner *et al.*, 1990). We will obtain results for the stress intensity factors and the energy release rate. In addition we will exhibit the range of applicability of the asymptotic solution for the sub-interface crack derived by Hutchinson *et al.* (1987). In our investigation of coated systems we will obtain the value of the critical thickness of the coating for which $K_{II} = 0$. We also note an interesting dependence of the stress intensity factors for the case of concentrated loading on the distance to the interface.

2. FORMULATION: TWO HALF-PLANES

The method of complex potentials (Muskhelishvili, 1953) provides an effective way to solve the stress field induced by the presence of a dislocation in a material. The stress field due to a dislocation near an interface, Fig. 1a, has been derived by Suo (1989); [see also Suo and Hutchinson (1990)] and the stress field due to this edge dislocation along $y = -ih$ is

$$\sigma_{yy} + i\sigma_{xy} = \frac{2\bar{B}}{\zeta} + BH_1(\zeta) + \bar{B}H_2(\zeta), \tag{1}$$

where $\zeta = x - \xi$, $\Lambda = (\alpha+\beta)/(1-\beta)$, $\Pi = (\alpha-\beta)/(1+\beta)$.

$$B = \frac{\mu_2}{\pi i(1+\kappa_2)}(b_1 + ib_2), \qquad H_1 = \frac{16\Pi\zeta h^2}{[\zeta^2+4h^2]^2},$$
$$H_2(\zeta) = \frac{(\Pi+\Lambda)\zeta - 2hi(\Pi-\Lambda)}{\zeta^2+4h^2} - \frac{8\Pi h^2}{[\zeta-2hi]^3}. \tag{2}$$

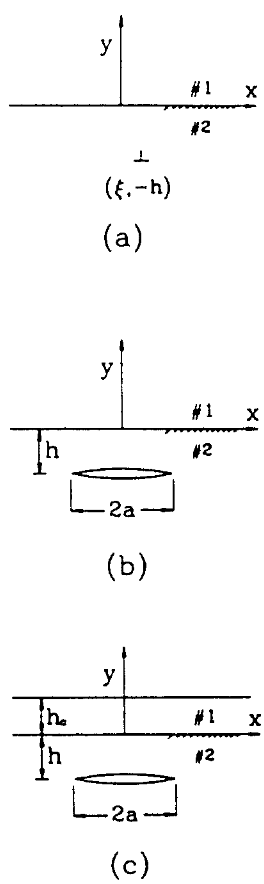

Fig. 1. (a) Edge dislocation near an interface. (b) Subinterface crack near the interface of two half-planes. (c) Subinterface crack under coating of thickness h_c.

where

$$\alpha = \frac{\mu_1(\kappa_2+1)-\mu_2(\kappa_1+1)}{\mu_1(\kappa_2+1)+\mu_2(\kappa_1+1)}$$

$$\beta = \frac{\mu_1(\kappa_2-1)-\mu_2(\kappa_1-1)}{\mu_1(\kappa_2+1)+\mu_2(\kappa_1+1)}$$

where the subscripts 1 and 2 refer to each of the two materials, $\kappa = 3-4\nu$ for plane strain and $(3-\nu)/(1+\nu)$ for plane stress, ν is Poisson's ratio, μ is the shear modulus, and h is the distance of the crack from the interface (Suo, 1989; Suo and Hutchinson, 1990). Along $z = x+iy$, $y > 0$ (material No. 1), we have

$$\sigma_{yy}+i\sigma_{xy} = B[(1+\Pi)h-(1+\Lambda)y]\frac{2i}{[\zeta+i(h+y)]^2}+\bar{B}\left\{\frac{1+\Lambda}{\zeta-i(h+y)}+\frac{1+\Pi}{\zeta+i(h+y)}\right\}. \quad (3)$$

A crack parallel to an interface or what we call a subinterface (Hutchinson *et al.*, 1987) crack has a crack tip singularity of order $r^{-1/2}$. Of particular interest is the amount of Mode II behavior at the crack tip to determine the subsequent direction of propagation from the crack tip. The subinterface crack as shown in Fig. 1b is modeled by continuously distributed edge dislocations along the crack of length $2a$. The interface is between two semi-infinite planes at $y = 0$ and the crack is located in material No. 2 below the surface. Using (1) after imposing the boundary condition that the traction on the crack faces is $\hat{p}(x)$, we obtain

$$2\int_{-a}^{a}\frac{\bar{B}(\xi)}{x-\xi}\,d\xi+\int_{-a}^{a}B(\xi)H_1(x-\xi)\,d\xi+\int_{-a}^{a}\bar{B}(\xi)H_2(x-\xi)\,d\xi = \hat{p}(x), \quad |x| < a. \quad (4)$$

In addition we have the condition

$$\int_{-a}^{a}B(\xi)\,d\xi = 0. \quad (5)$$

The integral equation (4) and condition (5) are non-dimensionalized with

$$\xi = at, \quad |t| < 1 \qquad x = au, \quad |u| < 1$$
$$B(\xi) = A(t) \quad \hat{p}(x) = p(u) \quad (6)$$

and take the forms

$$2\int_{-1}^{1}\frac{\bar{A}(t)}{u-t}\,dt+\int_{-1}^{1}A(t)H_1(x-\xi)a\,dt+\int_{-1}^{1}\bar{A}(t)H_2(x-\xi)a\,dt = p(u), \quad |u| < 1 \quad (7)$$

$$\int_{-1}^{1}A(t)\,dt = 0. \quad (8)$$

The integral equation (7) can be solved numerically by the techniques used for example by Erdogan (1969), Erdogan *et al.* (1972), and the references cited above. Therefore, in the case of uniform pressure the dislocation density function $A(t)$ can be assumed to be of the form (Hutchinson *et al.*, 1987)

$$A(t) = \frac{1}{\sqrt{1-t^2}}\sum_{k=0}^{N}a_kT_k(t) \quad (9)$$

where $T_k(t)$ is the Chebyshev polynomial of the first kind. In the case when a concentrated load is applied on the surface of the crack at a point u_0, $p(u) = -P_0\delta(u-u_0)$, the presence of the Delta function in the loading gives rise to another singular point in the dislocation density corresponding to the point at which the concentrated load is applied. Therefore, the dislocation density function $A(t)$ for a concentrated load can be assumed in the form

$$A(t) = \frac{1}{\sqrt{1-t^2}}\left\{\frac{C}{t-u_0} + \sum_{k=0}^{N} a_k T_k(t)\right\} \tag{10}$$

where $a_0 = 0$ upon the use of (8) and

$$C = \frac{P_0}{2\pi^2 a}\sqrt{1-u_0^2} \tag{11}$$

to provide the correct singularity at $t = u_0$.

The governing equations for both loadings are given in Appendix A. The stress intensity factors are given by (A3) and (A4) along with the energy release rate in (A5).

The $2N$ unknowns in (A1) of Appendix A, the real and imaginary parts of a_k, can be solved so that the real and imaginary parts of (A1) are satisfied at N selected collocation points u_i on the interval $|u| < 1$. We have used the Gauss–Legendre points for u_i in our numerical work (Erdogan *et al.*, 1972).

The numerical solutions were carried out using the IMSL software, and the major effort in the solution process was to accurately evaluate all the improper integrals. The integrals I_1 and I_2 in (A2) have end point singularities, and they were evaluated by the subroutine DQDAG. The integral that appears on the right side of (A1) has a singular point at the location of the concentrated load in addition to the end point singularities and it was evaluated by the subroutine DQDAWC.

The convergence of the solutions depends on the normalized crack-to-interface distance $\rho = h/a$. For small ρ, typically $\rho < 0.1$, the convergence of the solution requires a large number of integration points as discussed by Lu (1991). We have generated solutions for ρ as small as 0.01 for the uniform pressure loading and 0.05 for the concentrated loading. We note that for small values of ρ, Hutchinson's asymptotic solutions (Hutchinson *et al.*, 1987) for a subinterface crack can be used and we will show that our solutions converge to Hutchinson's asymptotic solutions for small ρ.

3. NUMERICAL RESULTS AND DISCUSSION

The numerical results for the stress intensity factors $K_{\rm I}$, $K_{\rm II}$ and the energy release rate G are presented by normalizing them with respect to the corresponding values of the homogeneous material No. 2. The results for the case of uniform pressure loading are shown in Figs 2–4. When the crack is far away from the interface, the results reduce to the results for the homogeneous case as we anticipate.

When material No. 1 is stiffer than material No. 2, $\alpha > 0$, the positive values of $K_{\rm II}$ as shown in Fig. 3 indicate that subsequent cracks propagating from the crack tips tend to propagate away from the interface. A corresponding argument holds when material No. 1 is softer than material No. 2, $\alpha < 0$, and the negative values of $K_{\rm II}$ indicate that the crack will propagate toward the interface. In the special case for material No. 1 being infinitely compliant, $\alpha = -1.0$, the crack is approaching a free surface, and the stress intensity factors and the energy release rate increase to infinity.

The results shown in Figs 2–4 approach to Hutchinson's subinterface asymptotic solutions (Hutchinson *et al.*, 1987) when the crack is very close to the interface, $h/a < 0.05$. Further we see that for $\alpha > -0.6$ (recall that the physical range of α is $-1.0 \leqslant \alpha \leqslant 1.0$, with β equal to 0), the asymptotic results are surprisingly accurate to values as high as $h/a \approx 0.3$.

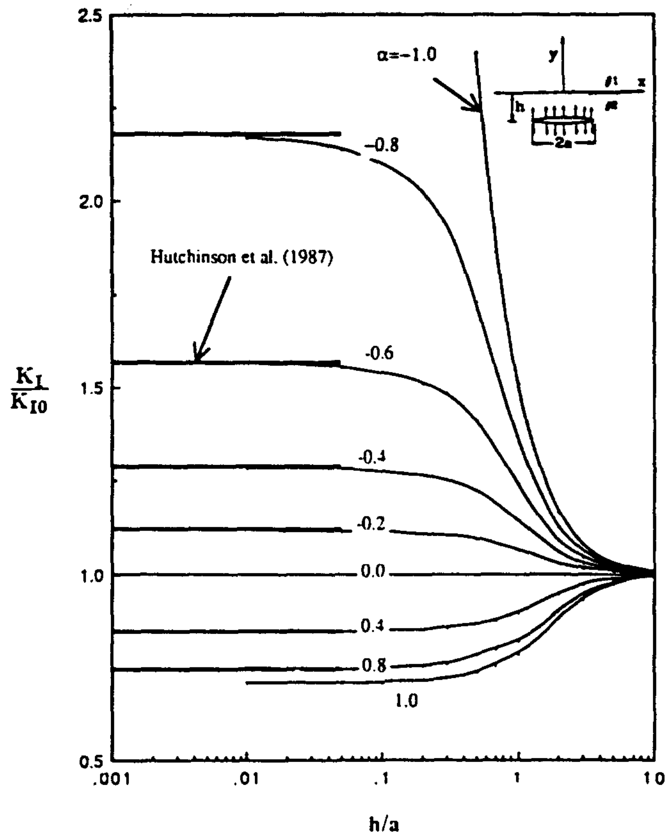

Fig. 2. Stress intensity factor K_I for cracks of length $2a$ under uniform pressure and parallel to an interface of two half-planes at a distance h; $\beta = 0$.

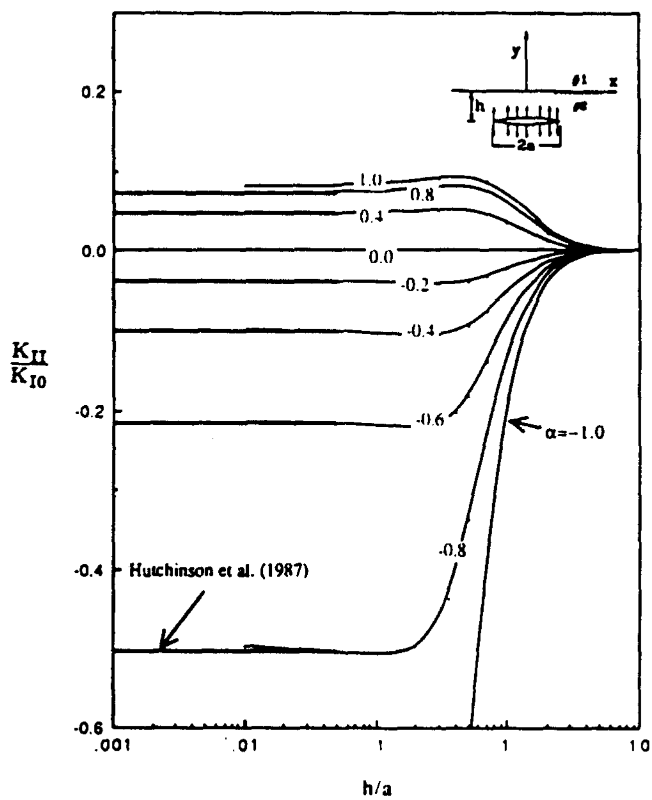

Fig. 3. Stress intensity factor K_{II} for cracks of length $2a$ under uniform pressure and parallel to an interface of two half-planes at a distance h; $\beta = 0$.

The results for the case of concentrated loadings are shown in Figs 5–7. It is seen that the stress intensity factors given in Figs 5 and 6 and the energy release rate given in Fig. 7 approach to a peak value and then decrease (or increase) to the asymptotic solutions when h/a is less than 0.1. This implies that under a pair of concentrated loads, the crack may or may not propagate depending on the fracture toughness of the material and the crack-to-interface distance, or equivalently on the crack length at a fixed distance from the interface. As suggested in Fig. 8, if the critical energy release rate of the material No. 2 is G_c, a crack under concentrated load will propagate if its length is between $2a_1$ and $2a_2$, otherwise it will remain stable. This phenomenon is especially notable when material No. 1 is very soft. We note that the peak values occur in the range $0.1 < h/a < 1$.

The effect of β on the stress intensity factors is shown in Figs 9 and 10. Again we see that the solutions approach the Hutchinson *et al.* (1987) subinterface solutions. The subinterface solution is surprisingly accurate up to values as high as $h/a = 0.10$.

4. SUBINTERFACE CRACKS UNDER COATINGS

This section is an extension of Sections 2 and 3 in which material No. 1 is now of finite thickness h_c so as to form a coating-substrate system as shown in Fig. 1c. We will focus on the effect of the thickness of the coating and the crack-to-interface distance on the stress intensity factors, the energy release rate and the direction of crack propagation. We will also consider the question of the critical thickness of the coating to ensure that the crack will propagate parallel to the interface (Hutchinson *et al.*, 1987).

Figure 11 shows the approach to be taken following Suo and Hutchinson (1989a). As depicted in Fig. 11, the solution to problem (i) where an edge dislocation with a Burger's vector $b = b_x + ib_y$ is located at $(0, -h)$ near the coating-substrate interface can be obtained

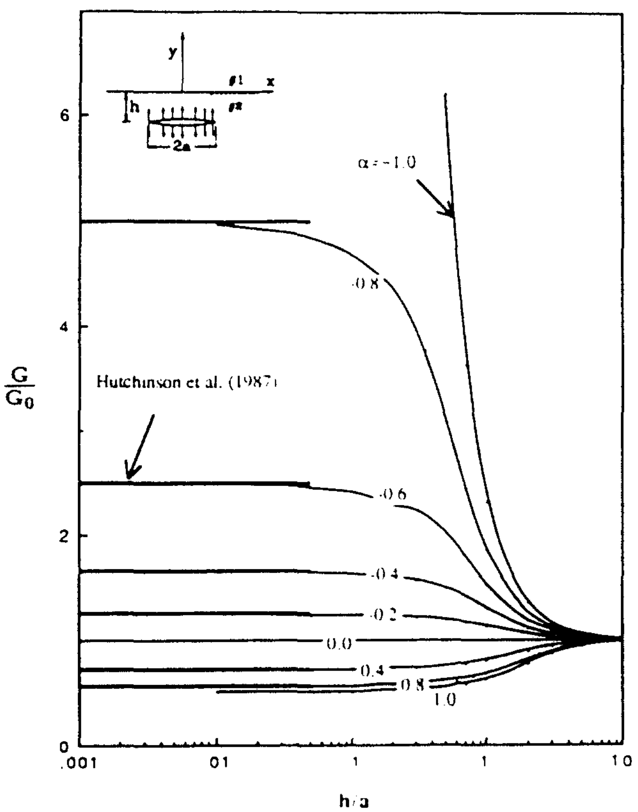

Fig. 4. Energy release rate G for cracks of length $2a$ under uniform pressure and parallel to an interface of two half-planes at a distance h; $\beta = 0$.

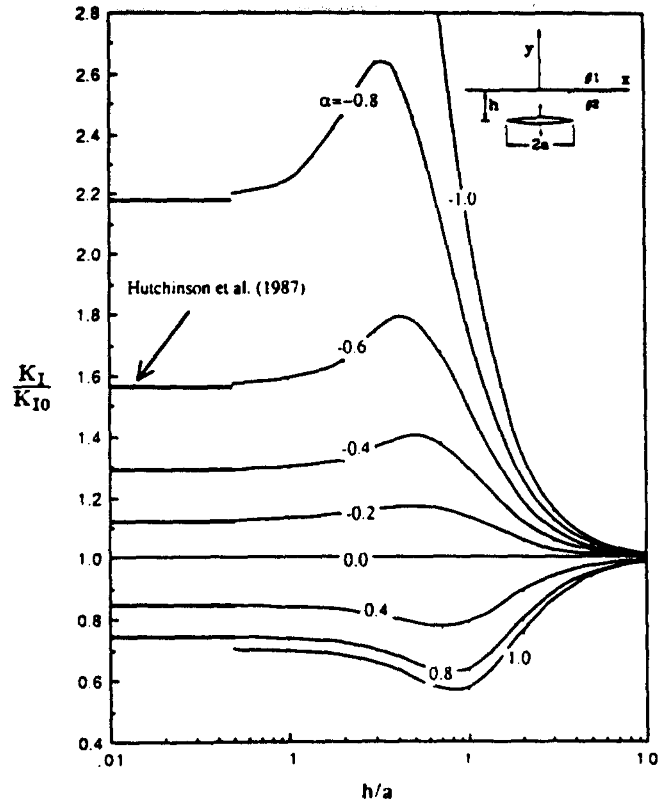

Fig. 5. Stress intensity factor K_I for cracks of length $2a$ under concentrated load and parallel to the interface of two half-planes at a distance h; $\beta = 0$.

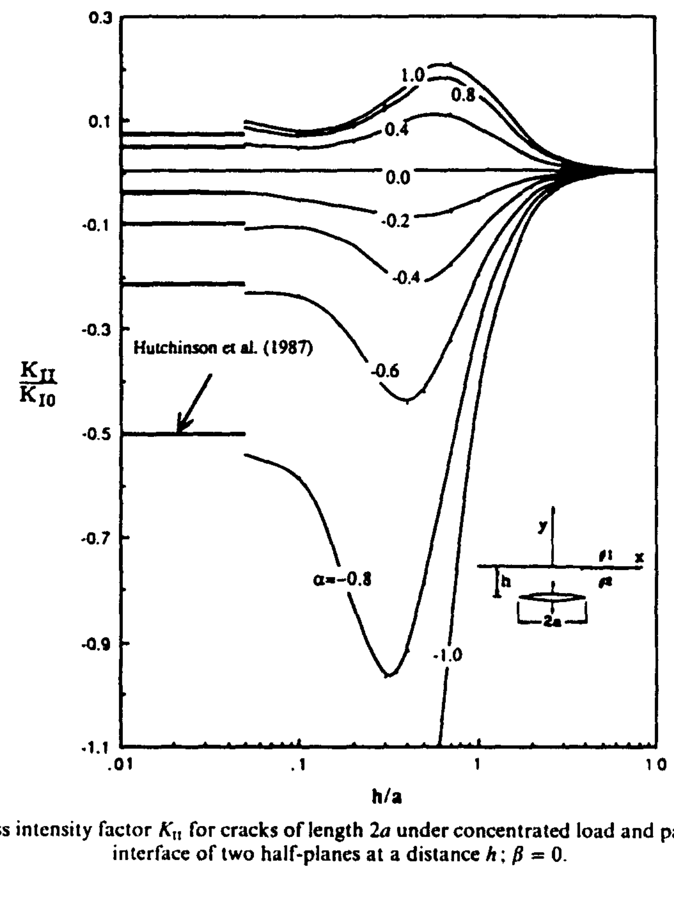

Fig. 6. Stress intensity factor K_{II} for cracks of length $2a$ under concentrated load and parallel to the interface of two half-planes at a distance h; $\beta = 0$.

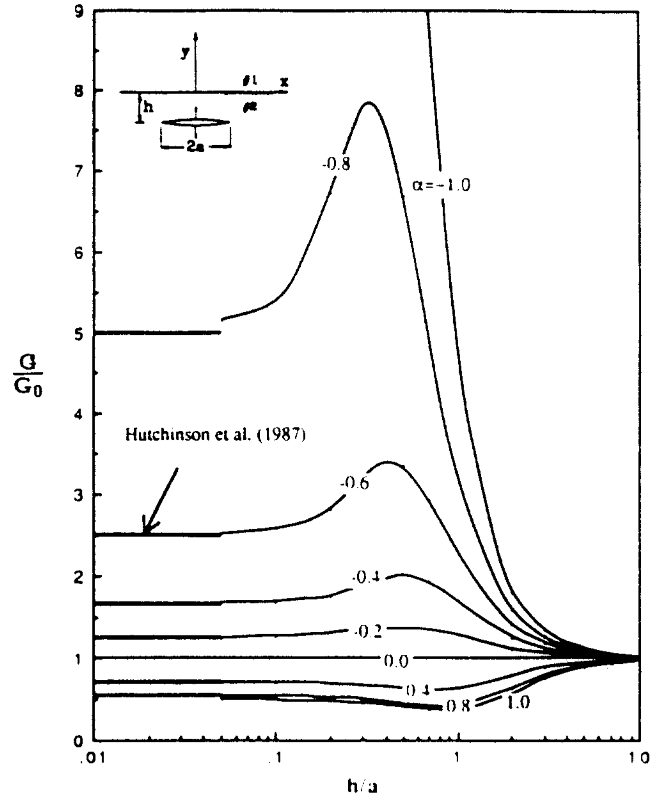

Fig. 7. Energy release rate G for cracks of length $2a$ under concentrated load and parallel to the interface of two half-planes at a distance h; $\beta = 0$.

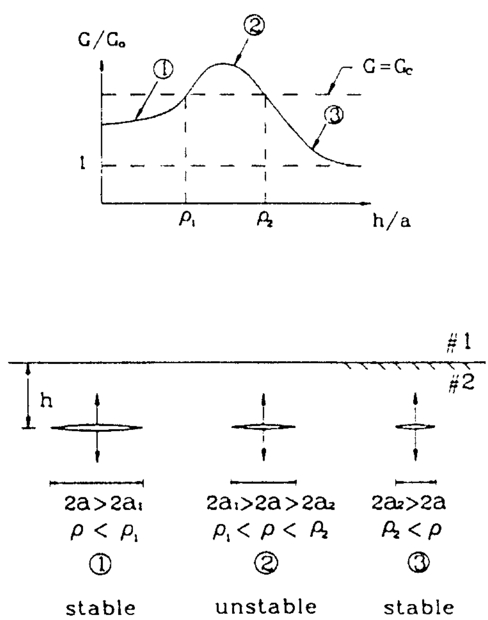

Fig. 8. Stability of cracks of length $2a$ under concentrated load and parallel to the interface of two half-planes at a distance h; $\alpha < 0$, $\beta = 0$.

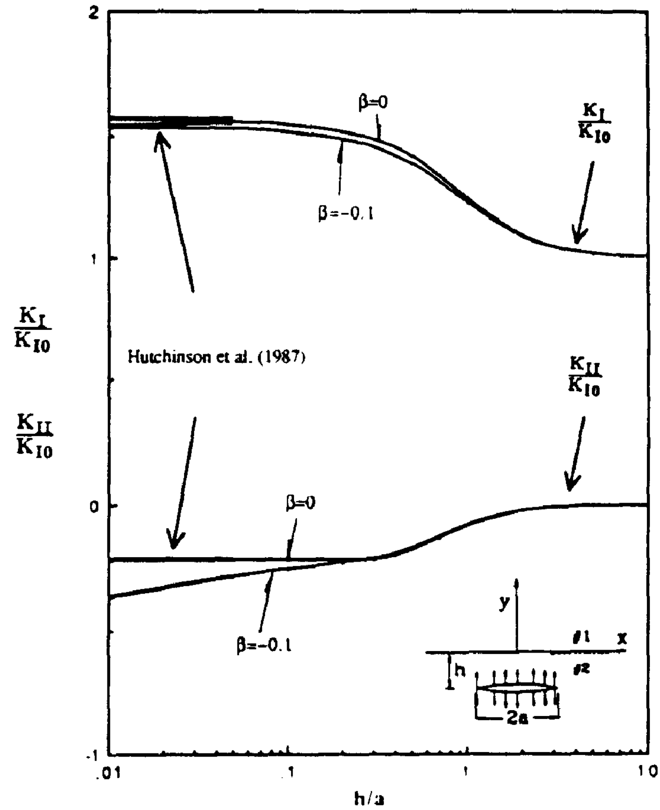

Fig. 9. Effect of β on the stress intensity factors for crack of length $2a$ under uniform pressure and parallel to the interface of two half-planes; $\alpha = -0.6$, $\beta = 0$ and -0.1.

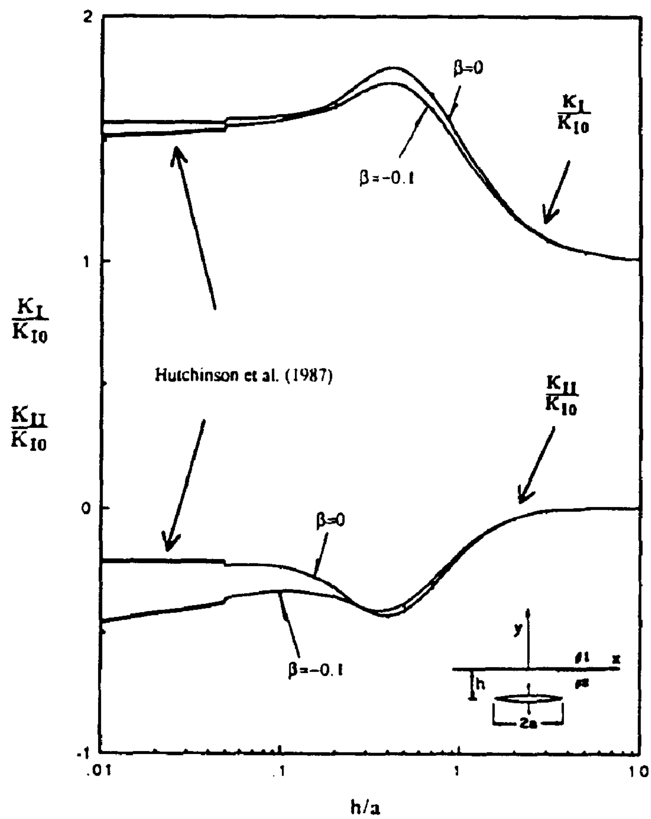

Fig. 10. Effect of β on the stress intensity factors for crack of length $2a$ under concentrated loading and parallel to the interface of two half-planes; $\alpha = -0.6$, $\beta = 0$ and -0.1.

by the superposition of the problems of (ii), an edge dislocation with a Burger's vector $b = b_x + ib_y$ at $(0, -h)$ near the interface of two half-planes and, (iii) the coating-substrate system without the edge dislocation but with an external traction $-\sigma^*(x)$ prescribed on the surface of the coating $y = h_c$, where $\sigma^*(x)$ are the stresses along $y = h_c$ calculated from problem (ii).

The stresses along $y = h_c$ in material No. 1 follow from (3) in the form:

$$\sigma_{yy}(x, h_c) + i\sigma_{xy}(x, h_c) = B[(1+\Pi)h - (1+\Lambda)y]\frac{2i}{[x+(h+h_c)]^2}$$
$$+\bar{B}\left\{\frac{1+\Lambda}{x-i(h+h_c)} + \frac{1+\Pi}{x+i(h+h_c)}\right\} \quad (12)$$

and the stresses along $y = -h$ in material No. 2 are given by (1).

The second problem is a traditional two-dimensional elasticity problem and can be solved by the use of stress functions and Fourier transforms as outlined by Suo and Hutchinson (1989a); detailed derivations of the solutions are given in Lu (1991). The stresses along $x = -h$ in material No. 2 are:

$$\sigma_{yy}(x, -h) + i\sigma_{xy}(x, -h) = BG_1(x) + \bar{B}G_2(x) \quad (13)$$

where $G_1(x)$ and $G_2(x)$ are given in Appendix B.

The formulation in terms of the dislocation density for the subinterface crack follows the steps given in Section 2 and we obtain a non-dimensional integral equation in the form:

$$2\int_{-1}^{1}\frac{A}{u-t}\,dt + \int_{-1}^{1}\bar{A}F_2(\zeta)a\,dt + \int_{-1}^{1}A(t)F_1(\zeta)a\,dt = p(u) \quad |u| < 1 \quad (14)$$

with the subsidiary equation

$$\int_{-1}^{1}A(t)\,dt = 0 \quad (15)$$

where

$$F_1(\zeta) = H_1(\zeta) + G_1(\zeta)$$
$$F_2(\zeta) = H_2(\zeta) + G_2(\zeta). \quad (16)$$

These results can be obtained from results in Suo and Hutchinson (1989a) upon setting H in their notation equal to infinity.

Following the same arguments as in Section 2, we assume the unknown function $A(t)$ as in (9) and (10) and the form of the resulting equations is given in Appendix C.

The accuracy of the solution depends on the evaluations of the integrals in (C2) to (C4). We note that the integrands of these integrals contain integral expressions G_1 and G_2. Therefore, the evaluation of the integrals requires greater care and computer time than the evaluation of the integrals in the previous section. The integrations were performed by the IMSL subroutines and the subroutine DQDAGI was used to evaluate the inner integrals G_1 and G_2 in the integrals I_1, I_2 and the right-hand side of (C2). The subroutines DQDAG and DQDAWC were then used to evaluate the integrals I_1 and I_2 and the right-hand side of (C2) respectively; see Lu (1991) for additional details. We have obtained the solutions for the stress intensity factors and the energy release rate for h as small as 0.2 using $N = 20$ and $N = 10$ for $h > 0.2$.

The direction of propagation of the crack is determined by the Mode II stress intensity factor K_{II}. We have seen from the results of Section 3 with two half planes that when material No. 1 is stiffer than material No. 2, $\alpha > 0$, the crack will propagate away from the interface, $K_{II} > 0$, under symmetric loading. In the case of a coating-substrate system, K_{II} is a function of the relative stiffness of the coating and the substrate as well as of the thickness of the coating.

When α is positive, K_{II} is negative when h_c is small and increases with an increase in the value of h_c. At a critical thickness h_{cr}, the stress intensity factor K_{II} becomes zero, and the crack will propagate parallel to the interface. This critical thickness of the coating depends explicitly on the relative stiffness of the system, α (with $\beta = 0$), and the crack-to-interface distance h as shown in Fig. 12. It is seen that h_{cr} increases as h decreases, and decreases as α increases. That is to say, the less stiff coatings need to be thicker if the crack is to propagate parallel to the interface. Furthermore, we see from Fig. 12 that the critical thickness of the coating is not sensitive to the external loading and is fairly constant for $0.5 < h/a < 1$.

The stress intensity factors and the energy release rate of the subinterface crack under uniform pressure and a pair of concentrated loads as functions of the crack-to-interface distance with $h_c = 0, 0.5, 1, 2, 4, \infty$ and with $\alpha = 0.8, 0.2$ and -0.2, $\beta = 0$ have been calculated, Lu (1991).

The responses of the coating-substrate system to the case of concentrated loading are similar to the case of uniform pressure; see Figs 13–15. For a crack under the pair of concentrated loads, the stress intensity factors if h_c is large enough reach a peak value before approaching a steady value when h/a is small.

The effect of the value of β on the stress intensity factors and the energy release rate is shown in Figs 16–18 in which the results for the coating-substrate system with $\alpha = 0.8$, $\beta = 0.0$ are compared to the coating-substrate system with $\alpha = 0.8$, $\beta = -0.2$ and 0.2. We found in general that the effect of β on the magnitude of the stress intensity factors and the

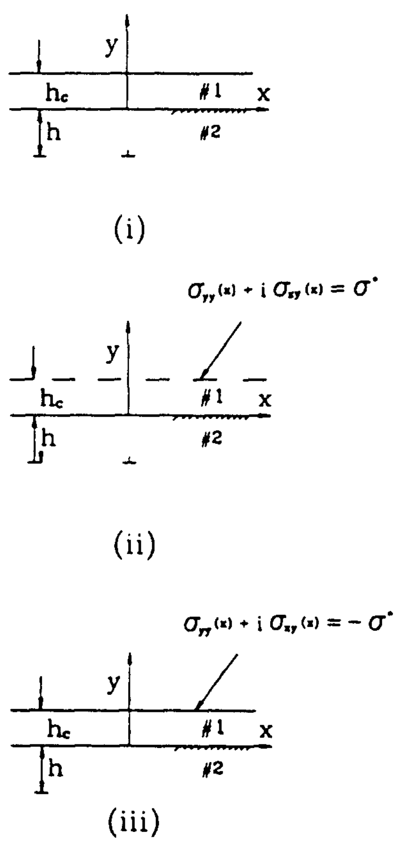

Fig. 11. Dislocation near a coating-substrate system. Problem (i) = (ii) + (iii).

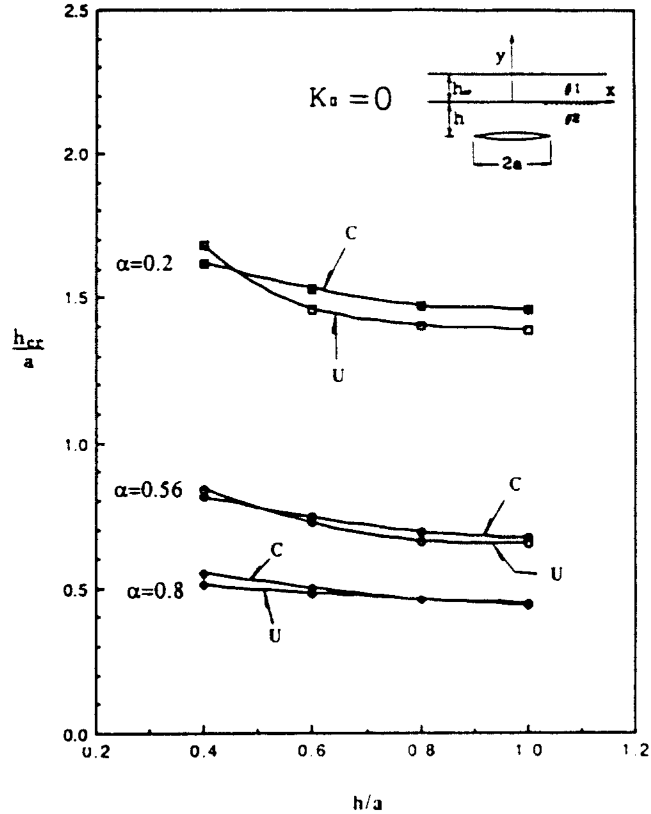

Fig. 12. Critical thickness h_{cr} of the coating ($K_{II} = 0$) for cracks of length $2a$ and parallel to a coating-substrate system at a distance h; $\beta = 0$; C: $p(x) = -P_0\delta(x)$, U: $p(x) = -p$.

energy release rate is not significant; results with $\beta = 0$ can be used as a good first estimate for the stress intensity factors and the energy release rate for a coating-substrate system with a subinterface crack.

5. CONCLUSIONS

We have investigated a number of problems for two-dimensional cracks near a bi-material interface. The major effort in the numerical solution was to accurately evaluate the improper integrals appearing in the singular integral equations. We used the IMSL package to carry out all the integrations and the numerical convergence of the integrals depends on the crack-to-interface distance.

We found that when the crack is embedded in the less stiff material of two half-planes, $\alpha > 0$, the normalized stress intensity factor K_I/K_{I0} and the normalized energy release rate G/G_0 are less than one for all values of the crack-to-interface distance. Conversely, when the crack is embedded in the stiffer material, $\alpha < 0$, K_I/K_{I0} and G/G_0 are greater than one for all values of the crack-to-interface distance. When $\alpha > 0$ the normalized stress intensity factor K_{II}/K_{I0} is positive so that the crack will propagate away from the interface, and when $\alpha < 0$, K_{II}/K_{I0} is negative so that the crack will propagate toward the interface.

We found that the stress intensity factors and the energy release rate approach to the asymptotic solution derived by Hutchinson *et al.* (1987) for both the case of uniform pressure loading and the concentrated loading when the crack is near to the interface. When the crack is under concentrated load, the stress intensity factors and the energy release rate reach a peak value before approaching their asymptotic values.

In the case of a finite thickness material on a half-plane we found that for a soft coating, $\alpha < 0$, K_I/K_{I0} and G/G_0 are always greater than one, and K_{II}/K_{I0} is always negative

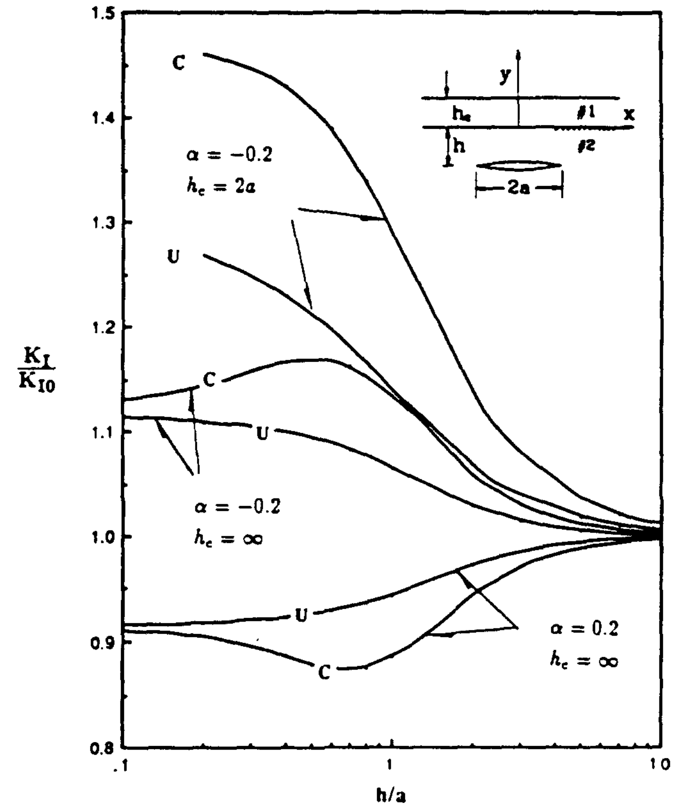

Fig. 13. Stress intensity factor K_I for the cases of concentrated loading and uniform pressure loading with $\alpha = -0.2, 0.2$, and $\beta = 0$; C: $p(x) = -P_0\delta(x)$, U: $p(x) = -p$.

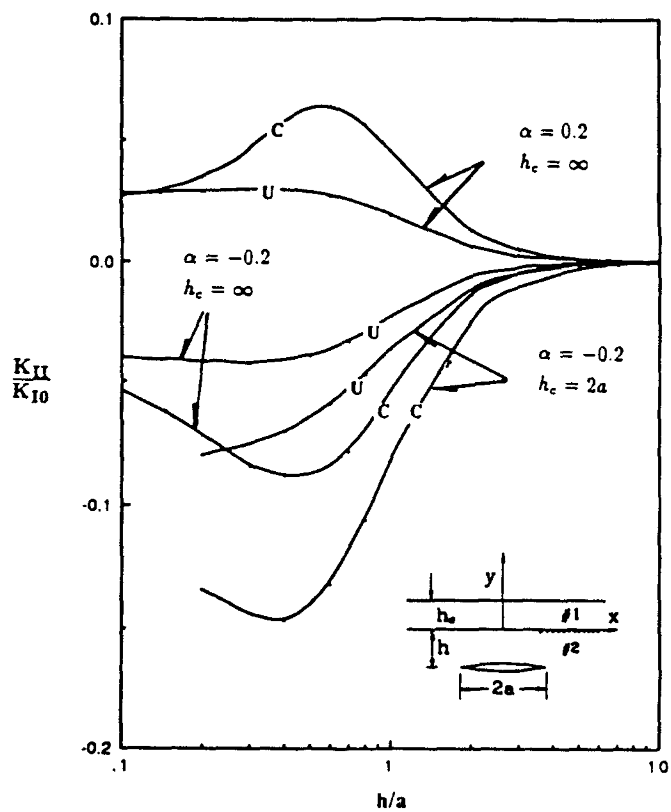

Fig. 14. Stress intensity factor K_{II} for the cases of concentrated loading and uniform pressure loading with $\alpha = -0.2, 0.2$, and $\beta = 0$; C: $p(x) = -P_0\delta(x)$, U: $p(x) = -p$.

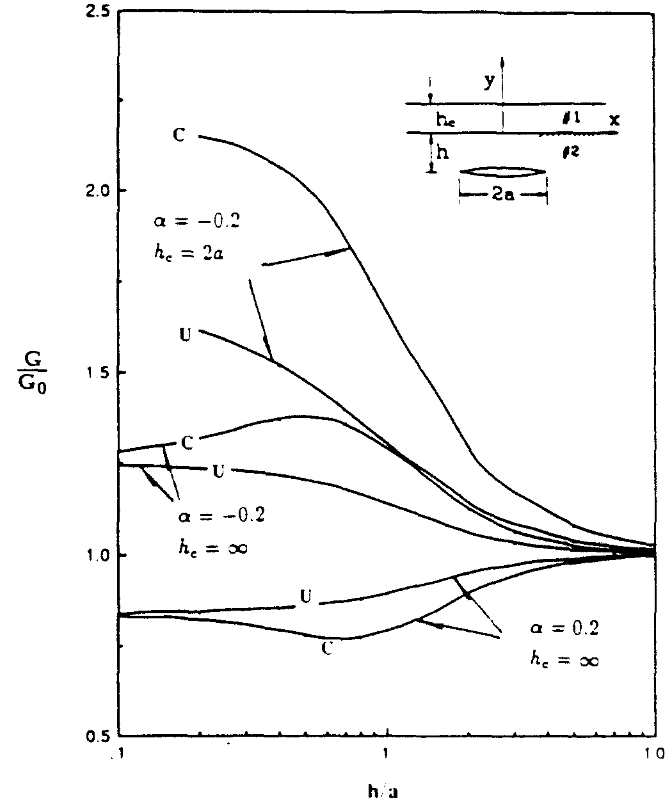

Fig. 15. Energy release rate G for the cases of concentrated loading and uniform pressure loading with $\alpha = -0.2$, 0.2, and $\beta = 0$; C: $p(x) = -P_0\delta(x)$, U: $p(x) = -p$.

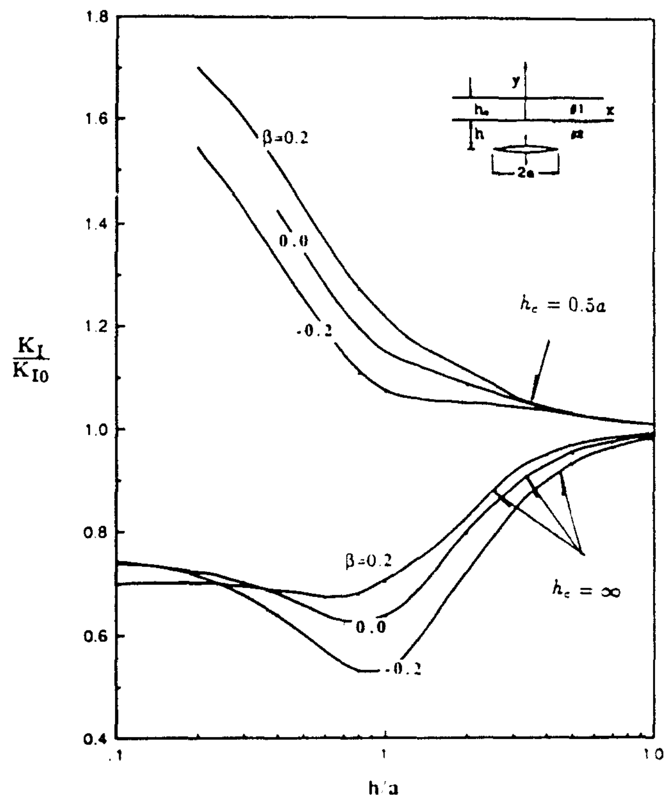

Fig. 16. Effect of β on the stress intensity factor K_I; $\alpha = 0.8$, $\beta = -0.2$, 0.0 and 0.2; concentrated loading.

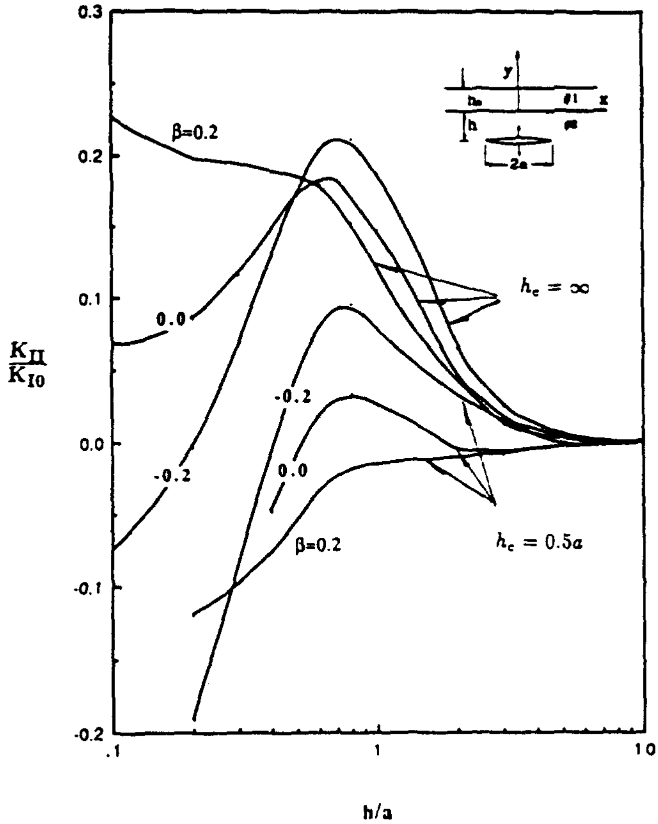

Fig. 17. Effect of β on the stress intensity factor K_{II}; $\alpha = 0.8$, $\beta = -0.2$, 0.0 and 0.2; concentrated loading.

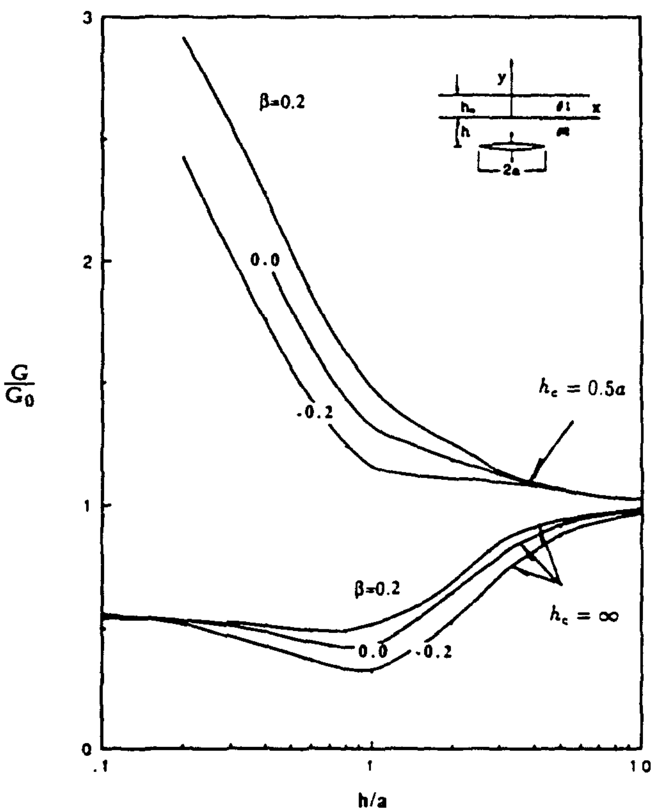

Fig. 18. Effect of β on the energy release rate G; $\alpha = 0.8$, $\beta = -0.2$, 0.0 and 0.2; concentrated loading.

for all thicknesses of the coating h_c and crack-to-interface distance h. That is, soft coatings regardless of their thickness are not likely to provide reinforcement to the cracked substrate and the crack will propagate toward the interface.

For a stiff coating, K_{II}/K_{I0} can be positive or negative depending on the thickness of the coating; that is, whether the crack will propagate away or toward the interface depends on the thickness of the coating. At a critical thickness of the coating, h_{cr}, where $K_{II} = 0$, the crack will propagate parallel to the interface. The magnitude of the critical thickness of the coating decreases as the coating becomes stiffer and increases as the crack-to-interface distance h decreases. We find that the critical thickness of the coating is not sensitive to the external loading on the crack and is fairly constant for $0.5 < h/a < 1$. When the thickness of the coating is greater than the critical thickness of the coating, $h > h_{cr}$, K_I/K_{I0} and G/G_0 are less than one for all values of the crack-to-interface distance.

The effect of β on the stress intensity factors appears to be not significant over the range of parameters we considered.

Acknowledgements—Part of this work was supported by an IBM grant to the Institute for Interface Science at the University of Massachusetts at Amherst and by NSF grant DMR-8919374.

REFERENCES

Ashbaugh, N. (1975). Stress solution for a crack at an arbitrarily oriented crack. *Int. J. Solids Structures* **10**, 569–685.

Bilby, B. and Eshelby, J. D. (1968). Dislocations and the theory of fracture. In *Fracture, An Advanced Treatise* (Edited by H. Liebowitz), Vol. I, pp. 99–182. Academic Press, New York.

Bogy, D. G. (1971). On the plane elastostatic problem of a loaded crack terminating at a material interface. *J. Appl. Mech.* **38**, 911–918.

Chen, B. (1991). Investigation of two-dimensional cracks at an angle to an interface. Ph.D. Dissertation, University of Massachusetts.

Cherepanov, G. P. (1979). *Mechanics of Brittle Fracture*. McGraw-Hill, New York.

Comninou, M. (1979). A closed crack tip terminating at an interface. *J. Appl. Mech.* **46**, 97–100.

Comninou, M. (1990). An overview of interface cracks. *Engng Fract. Mech.* **37**(1), 197–208.

Cook, R. F. and Pharr, G. M. (1990). Direct observation and analysis of indentation cracking in glasses and ceramics. *J. Am. Ceram. Soc.* **73**, 787–817.

England, A. H. (1965). A crack between dissimilar media. *J. Appl. Mech.* **32**, 400–402.

Erdogan, F. (1963). Stress distribution in a nonhomogeneous elastic plane with cracks. *J. Appl. Mech.* **30**, 232–236.

Erdogan, F. (1965). Stress distribution in bonded dissimilar materials with cracks. *J. Appl. Mech.* **32**, 403–410.

Erdogan, F. (1969). Approximate solution of singular integral equations. *SIAM J. Appl. Math.* **17**, 1041–1059.

Erdogan, F. and Arin, K. (1975). Half plane and a strip with an arbitrary located crack. *Int. J. Fract.* **11**, 191–204.

Erdogan, F., Gupta, G. D. and Cook, T. S. (1972). Numerical solution of singular integral equations. In *Methods of Analysis and Solutions of Crack Problems* (Edited by G. C. Sih), Vol. 1, pp. 368–425. Noordhoff, Gronigen, Holland.

Evans, A. G., Lu, M. C., Schmauder, S. and Ruhle, M. (1986). Some aspects of the mechanical strength of ceramic metal bonded systems. *ACTA Met.* **34**, 1643–1655.

Fenner, D. N. (1976). Stress singularities in composite material with an arbitrary oriented crack meeting an interface. *Int. J. Fract.* **12**(5), 705–721.

He, M. Y. and Hutchinson, J. W. (1988). Kinking of a crack out of an interface. *J. Appl. Mech.* **56**, 270–278.

He, M. Y. and Hutchinson, J. W. (1989). Crack deflection at an interface between dissimilar elastic materials. *Int. J. Solids Structures* **25**, 1053–1067.

Hutchinson, J. W., Mear, M. E. and Rice, J. R. (1987). Crack paralleling an interface between dissimilar materials. *J. Appl. Mech.* **54**, 828–832.

Hutchinson, J. W. and Suo, Z. (1991). Mixed mode cracking in layered materials. *Adv. Appl. Mech.* **28** (in press).

Lardner, T. J., Ritter, J. E. Shiao, M. L. and Lin, M. R. (1990). Behavior of cracks near free surfaces and interfaces. *Int. J. Fract.* **44**(2), 133–143.

Lu, H. (1991). Cracks on or near an interface. Ph.D. Dissertation, University of Massachusetts.

Lu, M. C. and Erdogan, F. (1983a). Stress intensity factors in two bonded elastic layers containing cracks perpendicular to and on the interface—I. Analysis. *Engng Fract. Mech.* **18**, 491–506.

Lu, M. C. and Erdogan, F. (1983b). Stress intensity factors in two bonded elastic layers containing cracks perpendicular to and on the interface—II. Solution and Results. *Engng Fract. Mech.* **18**, 507–528.

Lu, H. and Lardner, T. J. (1991). A note on the interface crack. *J. Appl. Mech.* (in press).

Malyshev, B. M. and Salganik, R. L. (1965). The strength of adhesive joints using the theory of cracks. *Int. J. Fract.* **1**, 114–128.

Muskhelishvili, N. I. (1953). *Some Basic Problems of the Mathematical Theory of Elasticity*. Noordhoff, Holland.

Ostojic, P. and McPherson, R. (1987). A review of indentation fracture theory: its development, principles and limitations. *Int. J. Fract.* **33**, 297–312.

Rice, J. (1968). Mathematical analysis in the mechanics of fracture. In *Fracture, An Advanced Treatise* (Edited by H. Liebowitz), Vol. II. Academic Press, New York.

Rice, J. R. (1988). Elastic fracture mechanics concepts for interfacial cracks. *J. Appl. Mech.* **55**, 98–103.
Rice, J. R. and Sih, G. C. (1965). Plane problems of cracks in dissimilar media. *J. Appl. Mech.* **32**, 418–423.
Suo, Z. (1989). Singularities interacting with interfaces and cracks—I. Isotropic materials. *Int. J. Solids Structures* **25**, 1133–1142.
Suo, Z. and Hutchinson, J. W. (1989a). Steady-state cracking in brittle substrates beneath adherent films. *Int. J. Solids Structures* **25**, 1337–1353.
Suo, Z. and Hutchinson, J. W. (1989b). Sandwich specimens for measuring interface crack toughness. *J. Mater. Sci. Engng* **A107**, 135–143.
Suo, Z. and Hutchinson, J. W. (1990). Interface crack between two elastic layers. *Int. J. Fract.* **43**, 1–18.
Thouless, M. D., Evans, A. G., Ashby, M. F. and Hutchinson, J. W. (1987). The edge cracking and spalling of brittle plates. *ACTA Met.* **35**, 1333–1341.
Williams, M. L. (1959). The stresses around a fault or crack in dissimilar media. *Bull. Seismol. Soc. America* **49**, 199–204.

APPENDIX A

For cracks near the interface of two half-planes, the form of the dislocation density function $A(t)$ is assumed as (9) when the crack is under uniform pressure, and in the form of (10) when the crack is under a pair of concentrated loads. Equation (8) then gives $a_0 = 0$ and the integral equation (7) becomes an algebraic equation of the form

$$-2\pi \sum_{k=1}^{N} \bar{a}_k U_{k-1} + \sum_{k=1}^{N} I_1(u,k) + \sum_{k=1}^{N} \bar{a}_k I_2(u,k)$$

$$= -p_0 \qquad \text{—for uniform pressure}$$

$$= -C\left\{\int_{-1}^{1} \frac{H_1(\zeta)+H_2(\zeta)}{\sqrt{1-t^2}(t-u_0)}\, a\,\mathrm{d}t\right\} \text{—for concentrated load} \tag{A1}$$

where

$$I_1(u,k) = -16\rho^2\Pi \int_{-1}^{1} \frac{t-u}{[(t-u)^2+4\rho^2]^2}\, \frac{T_k(t)}{\sqrt{1-t^2}}\,\mathrm{d}t$$

$$I_2(u,k) = \int_{-1}^{1} \frac{(\Pi+\Lambda)(u-t)-\mathrm{i}2\rho(\Pi-\Lambda)}{(u-t)^2+4\rho^2}\, \frac{T_k(t)}{\sqrt{1-t^2}}\,\mathrm{d}t - 8\Pi\rho^2 \int_{-1}^{1} \frac{T_k(t)\,\mathrm{d}t}{(u-t-\mathrm{i}2\rho)^3\sqrt{1-t^2}} \tag{A2}$$

and $\rho = h/a$.

The stress intensity factors are then obtained in terms of the dislocation density function in the form (Hutchinson *et al.*, 1987),

$$\bar{K} = 2\pi\sqrt{\pi a} \sum_{k=1}^{N} a_k \tag{A3}$$

for the case of uniform pressure loading, and

$$\bar{K} = 2\pi\sqrt{\pi a}\left\{\frac{C}{1-u_0} + \sum_{k=1}^{N} a_k\right\} \tag{A4}$$

for the case of concentrated loading.

The energy release rate is given by

$$G = \frac{\kappa_2+1}{8\mu_2} K\bar{K} \tag{A5}$$

APPENDIX B

The two-dimensional elasticity problem for a coating-substrate system under the loading $-\sigma^*(x)$ on the surface of the coating is considered briefly in this appendix; see Fig. 11. In particular, we are interested in the stress field along $y = -h$ in the substrate (Suo and Hutchinson, 1989a).

The problem is solved using stress functions for the stresses and displacements and Fourier transforms as outlined by Suo and Hutchinson (1988); see Lu (1991),

$$\Delta^2 U = 0, \quad \Delta\chi = 0, \quad \frac{\partial^2\chi}{\partial x\,\partial y} = \tfrac{1}{4}\Delta U. \tag{B1}$$

The stresses and displacements in terms of two real potentials are given by

$$\sigma_{xx} = \frac{\partial^2 U}{\partial^2 y}, \quad \sigma_{yy} = \frac{\partial^2 U}{\partial^2 x}, \quad \sigma_{xy} = -\frac{\partial^2 U}{\partial x \partial y} \tag{B2}$$

$$2\mu u_x = -\frac{\partial U}{\partial x} + (\kappa+1)\frac{\partial \chi}{\partial y} \tag{B3}$$

$$2\mu u_y = -\frac{\partial U}{\partial x} + (\kappa+1)\frac{\partial \chi}{\partial x}. \tag{B4}$$

The Fourier transform of $U(x, y)$ satisfying the biharmonic equation for each material is assumed in the forms (Suo and Hutchinson, 1988):

$$\bar{U}_1(\lambda, y) = \left[\frac{A_1}{\lambda^2} + \frac{A_2}{\lambda}y\right]e^{-|\lambda|y} + \left[\frac{A_3}{\lambda^2} + \frac{A_4}{\lambda}y\right]e^{\lambda y} \tag{B5}$$

$$\bar{U}_2(\lambda, y) = \left[\frac{B_1}{\lambda^2} + \frac{B_2}{\lambda}y\right]e^{-|\lambda|y} \tag{B6}$$

where

$$\bar{U}_i(\lambda, y) = \mathscr{F}\{U(x,y)\} = \int_{-\infty}^{\infty} U_i(x,y)\,e^{i\lambda x}\,dx, \quad i = 1,2 \tag{B7}$$

is the Fourier transform of $U_i(x, y)$.

The six constants A_1, A_2, A_3, A_4, B_1 and B_2 are to be determined from the boundary conditions that the stresses and displacements are continuous across the interface ($y = 0$) and the traction on the surface of the coating ($y = h_c$) is prescribed as $-\sigma^*(x) = -\sigma^*_{yy}(x) - i\sigma^*_{xy}(x)$.

The boundary and continuity equations lead to

$$A_1 + A_3 = B_1 \tag{B8}$$

$$-\frac{A_1}{|\lambda|} + \frac{A_2}{\lambda} + \frac{A_3}{|\lambda|} + \frac{A_4}{\lambda} = \frac{B_1}{|\lambda|} + \frac{B_2}{\lambda} \tag{B9}$$

$$A_1 - \frac{|\lambda|}{2\lambda}c_1A_2 + A_3 + \frac{|\lambda|}{2\lambda}c_1A_4 = \Gamma\left\{B_1 + \frac{|\lambda|}{2\lambda}c_2B_2\right\} \tag{B10}$$

$$-\frac{A_1}{|\lambda|} + \frac{2-c_1}{2\lambda}A_2 + \frac{A_3}{|\lambda|} + \frac{2-c_2}{2\lambda}A_4 = \Gamma\left\{\frac{B_1}{|\lambda|} + \frac{2-c_2}{2\lambda}B_2\right\} \tag{B11}$$

$$[A_1 + A_2\lambda h_c]\,e^{-|\lambda|h_c} + [A_3 + \lambda h_c A_4]\,e^{|\lambda|h_c} = \bar{\sigma}^*_{yy} \tag{B12}$$

$$\left[-\frac{\lambda}{|\lambda|}A_1 + A_2(1-|\lambda|h_c)\right]e^{-|\lambda|h_c} + \left[\frac{\lambda}{|\lambda|}A_3 + A_4(1+|\lambda|h_c)\right]e^{|\lambda|h_c} = i\bar{\sigma}^*_{xy} \tag{B13}$$

where $c_1 = \kappa_1 + 1$, $c_2 = \kappa_2 + 1$ and $\Gamma = \mu_2/\mu_1$.

Solving the system of equations for A_1, A_2, A_3 and A_4 in terms of B_1 and B_2 we obtain

$$\begin{bmatrix} P_{11} & P_{12} \\ P_{21} & P_{22} \end{bmatrix}\begin{Bmatrix} B_1 \\ B_2 \end{Bmatrix} = \begin{Bmatrix} \bar{\sigma}^*_{yy}(\lambda) \\ -i\bar{\sigma}^*_{xy}(\lambda) \end{Bmatrix} \tag{B14}$$

where

$$P_{11} = -(\alpha-\beta)(1+2\lambda h_c)\,e^{-\lambda h_c} + (1-\beta)\,e^{\lambda h_c} \tag{B15}$$

$$P_{12} = [\beta - (\alpha-\beta)\lambda h_c]\,e^{-\lambda h_c} - [\beta - (\beta+1)\lambda h_c]\,e^{\lambda h_c} \tag{B16}$$

$$P_{21} = (\alpha-\beta)(1-2\lambda h_c)\,e^{-\lambda h_c} + (\beta-1)\,e^{\lambda h_c} \tag{B17}$$

$$P_{22} = [\alpha - (\alpha-\beta)\lambda h_c]\,e^{-\lambda h_c} - [1 + (\beta+1)\lambda h_c]\,e^{\lambda h_c}. \tag{B18}$$

Equation (B14) provides a system of equations to solve for B_1 and B_2 under the loadings σ^*_{yy} and σ^*_{xy}. For the purpose of algebraic convenience, B_1 and B_2 are obtained by the superposition of the solutions taking the loading to be symmetric and anti-symmetric. That is,

$$\begin{bmatrix} P_{11} & P_{12} \\ P_{21} & P_{22} \end{bmatrix}\begin{Bmatrix} B_1 \\ B_2 \end{Bmatrix} = \begin{Bmatrix} \bar{\sigma}^*_{yys}(\lambda) \\ -i\bar{\sigma}^*_{xya}(\lambda) \end{Bmatrix} + \begin{Bmatrix} \bar{\sigma}^*_{yya}(\lambda) \\ -i\bar{\sigma}^*_{xys}(\lambda) \end{Bmatrix} \tag{B19}$$

where the subscripts a and s stand for the anti-symmetric and symmetric parts of the stress σ^*_{yy} and σ^*_{xy}.

The traction $\sigma^*(x)$ can be written as

$$\sigma^*(x) = \sigma^*_{yy} + i\sigma^*_{xy}(x) = [\sigma^*_{yys}(x) + \sigma^*_{yya}(x)] + i[\sigma^*_{xys}(x) + \sigma^*_{xya}]$$

where

$$\sigma^*_{yys}(x) = \frac{B-\bar{B}}{2\mathrm{i}}\left\{\frac{4R_1H^2}{(x^2+H^2)^2} - \frac{2R_1+(R_2-R_3)H}{x^2+H^2}\right\}$$

$$\sigma^*_{yya}(x) = \frac{B+\bar{B}}{2}\left\{\frac{4R_1Hx}{(x^2+H^2)^2} + \frac{(R_2+R_3)x}{x^2+H^2}\right\}$$

$$\sigma^*_{xys}(x) = \frac{B+\bar{B}}{2}\left\{\frac{-4R_1H^2}{(x^2+H^2)^2} + \frac{2R_1-(R_2-R_3)x}{x^2+H^2}\right\}$$

$$\sigma^*_{xya} = \frac{B-\bar{B}}{2\mathrm{i}}\left\{\frac{4R_1Hx}{(x^2+H^2)^2} - \frac{(R_2+R_3)x}{x^2+H^2}\right\}$$

$$H = h+h_c$$

$$R_2 = 1+\Pi$$

$$R_3 = 1+\Lambda$$

$$R_1 = R_2h+R_3h_c.$$

We note that under symmetric loading the stress function $U_2(x, y)$ must be symmetric in x; therefore its Fourier transform must be symmetric in λ. Therefore, from (B7) we see B_1 must be symmetric in λ and B_2 must be anti-symmetric in λ. Similarly, under anti-symmetric loading $\bar{U}_2(\lambda, y)$ must be anti-symmetric in λ, and B_1 must be anti-symmetric in λ and B_2 must be symmetric in λ.

Therefore, (B14) can be rewritten in the form:

$$\begin{bmatrix} P_{11} & P_{12} \\ P_{21} & P_{22} \end{bmatrix}\begin{bmatrix} B_{1s} & B_{1a} \\ B_{2a} & B_{2s} \end{bmatrix} = \begin{bmatrix} \bar{\sigma}^*_{yys}(\lambda) & \bar{\sigma}^*_{yya}(\lambda) \\ -\mathrm{i}\bar{\sigma}^*_{xya}(\lambda) & -\mathrm{i}\bar{\sigma}^*_{xys}(\lambda) \end{bmatrix} \tag{B20}$$

where $B_1 = B_{1a}+B_{1s}$ and $B_2 = B_{2a}+B_{2s}$ and

$$\bar{\sigma}^*_{yys}(x) = 2\int_0^\infty \sigma^*_{yys}(x)\cos\lambda x\,\mathrm{d}x = -(B-\bar{B})\mathrm{i}\left[R_1\lambda - \frac{R_2-R_1}{2}\right]\pi\mathrm{e}^{-\lambda H}$$

$$\bar{\sigma}^*_{yya}(x) = 2\int_0^\infty \sigma^*_{yya}(x)\sin\lambda x\,\mathrm{d}x = (B+\bar{B})\left[R_1\lambda + \frac{R_2+R_1}{2}\right]\pi\mathrm{e}^{-\lambda H}$$

$$\bar{\sigma}^*_{xys}(x) = 2\int_0^\infty \sigma^*_{xys}(x)\cos\lambda x\,\mathrm{d}x = (B+\bar{B})\left[-R_1\lambda - \frac{R_2-R_1}{2}\right]\pi\mathrm{e}^{-\lambda H}$$

$$\bar{\sigma}^*_{xya}(x) = 2\int_0^\infty \sigma^*_{xya}(x)\cos\lambda x\,\mathrm{d}x = -(B-\bar{B})\mathrm{i}\left[R_1\lambda - \frac{R_2+R_1}{2}\right]\pi\mathrm{e}^{-\lambda H}.$$

Upon use of the inverse transform of $\bar{U}_2(\lambda, x)$ we have the stress function $U_2(x, y)$ as

$$U_2(x,y) = \frac{1}{2\pi}\int_{-\infty}^{\infty}\left[\frac{B_1}{\lambda^2}+\frac{B_2}{\lambda}y\right]\mathrm{e}^{|\lambda|y}\,\mathrm{e}^{-\mathrm{i}\lambda x}\,\mathrm{d}\lambda.$$

It follows that the stresses along $y = -h$ are

$$\sigma_{yy}(x,-h)+\mathrm{i}\sigma_{xy}(x,-h) = \frac{\partial^2 U_2}{\partial x^2} - \mathrm{i}\frac{\partial^2 U_2}{\partial x\,\partial y} = -\frac{1}{2\pi}\int_{-\infty}^{\infty}[B_1 - B_2\lambda h]\,\mathrm{e}^{-|\lambda|h}\,\mathrm{e}^{-\mathrm{i}\lambda x}\,\mathrm{d}\lambda$$

$$-\frac{1}{2\pi}\int_{-\infty}^{\infty}\left[\frac{|\lambda|}{\lambda}B_1 + B_2(1-|\lambda|h)\right]\mathrm{e}^{-|\lambda|h}\,\mathrm{e}^{-\mathrm{i}\lambda x}\,\mathrm{d}\lambda = \frac{1}{\pi}\int_0^\infty[-B_1 - B_{2s} + B_2\lambda h]\,\mathrm{e}^{-\lambda h}\cos\lambda x\,\mathrm{d}\lambda$$

$$+\frac{\mathrm{i}}{\pi}\int_0^\infty[B_1 + B_{2a} - B_2\lambda h]\,\mathrm{e}^{-\lambda h}\sin\lambda x\,\mathrm{d}\lambda. \tag{B21}$$

Substitution of B_{1a}, B_{1s}, B_{2a} and B_{2s} from (B20) into (B21) leads to the results:

$$\sigma_{yy}(x,-h)+\mathrm{i}\sigma_{xy}(x,-h) = BG_1(x)+\bar{B}G_2(x) \tag{B22}$$

where

$$G_1(\zeta) = G_{1s}(\zeta)+G_{1a}(\zeta)$$

$$G_2(\zeta) = G_{2s}(\zeta)+G_{2a}(\zeta)$$

and

$$G_{1r}(\zeta) = \int_0^\infty \{2(1-\alpha)[(1+\beta)R_2h_c+(1-\beta)(2R_2h+R_3h_c)]\lambda\,\mathrm{e}^{-2\lambda(h+h_c)}-4(1-\alpha)(\alpha-\beta)R_2h\lambda\,\mathrm{e}^{-2\lambda(2h_c+h)}\}\frac{\sin\lambda\zeta}{M}\,\mathrm{d}\lambda$$

$$G_{1i}(\zeta) = \int_0^\infty 2(1-\alpha)h_c[\beta(R_2+R_3)+R_2-R_3]\lambda\,\mathrm{e}^{-2\lambda(h+h_c)}\frac{\cos\lambda\zeta}{M}\,\mathrm{d}\lambda$$

$$G_{2r}(\zeta) = \int_0^\infty \{\{4(1-\alpha)[\beta(h_c-h)+h_c-h]R_1\lambda^2+(1-\alpha)[\beta(R_3-R_2)+R_2+R_3]\}\,\mathrm{e}^{-2\lambda(h+h_c)}$$

$$-4(1-\alpha)(\alpha-\beta)R_2h^2\lambda^2\,\mathrm{e}^{-2\lambda(h_c+h)}+(1-\alpha)[\beta(R_2-R_3)-\alpha(R_2+R_3)]\,\mathrm{e}^{-2\lambda(2h_c+h)}\}\frac{\sin\lambda\zeta}{M}\,\mathrm{d}\lambda$$

$$G_{2i}(\zeta) = \int_0^\infty \{\{4(1-\alpha)[\beta(h_c-h)+h_c+h]R_1\lambda^2+(1-\alpha)[\beta(R_2+R_3)+R_3-R_2]\}\,\mathrm{e}^{-2\lambda(h+h_c)}$$

$$-4(1-\alpha)(\alpha-\beta)R_2h^2\lambda^2\,\mathrm{e}^{-2\lambda(h_c+h)}-(1-\alpha)[\beta(R_2+R_3)+\alpha(R_3-R_2)]\,\mathrm{e}^{-2\lambda(2h_c+h)}\}\frac{\cos\lambda\zeta}{M}\,\mathrm{d}\lambda$$

$$M = \beta^2-1+\{2\alpha-2\beta^2+[4\alpha-4\beta^2+4\beta(\alpha-1)]h_c^2\lambda^2\}\,\mathrm{e}^{-2\lambda h_c}+(\beta^2-\alpha^2)\,\mathrm{e}^{-4\lambda h_c}.$$

APPENDIX C

For subinterface cracks under coatings, the form of the dislocation density function $A(t)$ is assumed as in (9) when the crack is under uniform pressure, and in the form of (10) when the crack is under a pair of concentrated loads.

Upon substitution of (9) and (10) into (14) we have

$$-2\pi\sum_{k=1}^{N}\bar{a}_kU_{k-1}+\sum_{k=1}^{N}I_1(u,k)+\sum_{k=1}^{N}\bar{a}_kI_2(u,k)$$

$$= -p_0 \qquad \text{—for uniform pressure} \tag{C1}$$

$$= -C\left\{\int_{-1}^{1}\frac{F_1(\zeta)+F_2(\zeta)}{\sqrt{1-t^2}(t-u_0)}a\,\mathrm{d}t\right\}\text{—for concentrated load} \tag{C2}$$

where

$$I_1(u,k) = \int_{-1}^{1}\frac{T_k(t)F_1(\zeta)a\,\mathrm{d}t}{\sqrt{1-t^2}} \tag{C3}$$

$$I_2(u,k) = \int_{-1}^{1}\frac{T_k(t)F_2(\zeta)a\,\mathrm{d}t}{\sqrt{1-t^2}} \tag{C4}$$

and $a_0 = 0$.

Equations (C1) and (C2) are solved to obtain the unknown coefficients a_k.